



The Society shall not be responsible for statements or opinions advanced in papers or discussion at meetings of the Society or of its Divisions or Sections, or printed in its publications. Discussion is printed only if the paper is published in an ASME Journal. Papers are available from ASME for 15 months after the meeting.

Printed in U.S.A.

Copyright © 1993 by ASME

THE OPERATIONAL STABILITY OF A CENTRIFUGAL COMPRESSOR AND ITS DEPENDENCE ON THE CHARACTERISTICS OF THE SUBCOMPONENTS

René Hunziker

Turbomachinery Laboratory
ETH Swiss Federal Institute of Technology Zurich
Switzerland

Georg Gyarmathy

Turbomachinery Laboratory
ETH Swiss Federal Institute of Technology Zurich
Switzerland

ABSTRACT

A centrifugal compressor was tested with three different diffusers with circular-arc vanes. The vane inlet angle was varied from 15° to 30°. Detailed static wall pressure measurements show that the pressure field in the diffuser inlet is very sensitive to flow rate. The stability limit regularly occurred at the flow rate giving the maximum pressure rise for the overall stage. Mild surge arises as a dynamic instability of the compression system. The analysis of the pressure rise characteristic of each individual subcomponent (impeller, diffuser inlet, diffuser channel,...) reveals their contribution to the overall pressure rise. The diffuser channels play an inherent destabilizing role while the impeller and the diffuser inlet are typically stabilizing. The stability limit was mainly determined by a change in the characteristic of the diffuser inlet. Further, the stability limit was found to be independent of the development of inducer-tip recirculation.

INTRODUCTION

It is common industrial practice to adapt the optimal range of operation of centrifugal impellers to different users by combining them with diffusers of different geometry. Also, variable geometry diffusers are widely used to satisfy customer demand for broad range. There is great interest in reducing the empiricism involved in these approaches by establishing criteria for the influence of key geometric factors on the stability limit of the stage, all the more since maximum efficiency in centrifugal compressors usually occurs close to this limit and therefore the

necessity of a surge margin results in a reduced operating efficiency.

Flow instabilities have been studied extensively. Rotating stall, a frequently observed flow phenomena, sometimes, but not necessarily, precedes surge. Experimental data with vaneless diffuser rotating stall is given for example in Jansen (1964), Abdelhamid (1983), Frigne and Van Den Braembussche (1984), Rieder (1987). Rotating stall occurring in the impeller is described for example in Frigne and Van Den Braembussche (1984), Ariga et al. (1987) and Kämmer and Rautenberg (1982, 1986). Another type of flow instability, mild surge, also has been observed prior to the occurrence of "deep" surge (Emmons et al. (1955), Amann et al. (1975)). Intermittent mild surge cycles can be part of the whole deep surge cycle (Toyama et al. (1977), Dean and Young (1977), Fink et al. (1991)). Greitzer (1981) reviews the literature concerning different types of instabilities and provides criteria for the static and dynamic stability of the system comprising the compressor, the piping and the user. Based on the physical mechanisms for dynamic instability various passive and active control concepts have been proposed or realized (Pinsley et al. (1990), Gysling et al. (1990), Simon et al. (1992)).

In the literature many parameters determining compressor stability have been advanced, see for example the review by Elder (1985). Some of these parameters concern the impeller, some the diffuser. Often the semi-vaneless space is stated as the most critical element of a centrifugal compressor stage where the flow breaks down if a critical level of diffusion or a critical value of pressure recovery is exceeded (e.g. Kenny (1972), Toyama et al. (1977), Came

and Herbert (1980), Elder and Gill (1985)). But such critical values are not able to explain surge line shifts caused solely by changes in the diffuser channel geometry (Japikse (1980), Clements and Art (1987)).

The above mentioned work of Greitzer (1981) points out that for simple compression systems with a sufficiently large B-parameter a simple stage-stability parameter based on empirical pressure rise versus flow rate data can be deduced. The criteria states that the limit of dynamic stability coincides with the maximum of the total-to-static pressure rise characteristic. This argument can be extended to the individual components of the stage, indicating the components which are potentially unstable (Dean (1974), Japikse (1984)). A typical unstable subcomponent is the diffuser channel.

In diffuser design the (laboratory) 2-dimensional diffuser data of Reneau et al. (1967) and Runstadler et al. (1975) are commonly used. They show the relationship of geometry, pressure recovery, stalled regimes and inlet blockage. Comparisons of radial diffuser channel data and 2-dimensional duct or pipe diffuser data show principal agreement but discrepancies exist in the level of pressure recovery (Yoshinaga et al. (1980), Japikse and Osborne (1986)). There are several reasons for these discrepancies, e.g. difference in aspect ratio or difference in turbulence structures. Also the range of blockage values typical of radial diffusers were not completely covered by the duct data and the inflow conditions may differ significantly.

Detailed measurements of wall pressure distributions and of flow velocity fields in radial diffusers (e.g. Krain (1981), Jansen (1982), Stein and Rautenberg (1987)) provide insight into the complex flow structures existing within the vaneless and semi-vaneless space. Investigations in isolated diffuser test rigs are reported in Baghdadi and McDonald (1975), Dutton et al. (1986), Filipenco (1991). Information on the overall performance of diffusers and diffuser subcomponents are given for example in Kenny (1972), Rodgers (1982), Japikse and Osborne (1986), Clements (1987).

NOMENCLATURE

English Letters

A	geometric area
A_{eff}	effective area
AS	diffuser aspect ratio ($AS = b/h_C$)
AR	diffuser area ratio
Bl	diffuser throat blockage
b	diffuser width (axial)

C_p	pressure recovery coefficient
D_p	pressure rise coefficient
d	diameter
h	diffuser channel height (perpendicular to a mean streamline)
L	length of diffuser vane
l	diffuser channel length
M_u	peripheral Mach number
p_{dyn}	dynamic pressure
p	pressure
R	gas constant
r	radius
T	temperature
t	diffuser vane thickness
u	circumferential speed
\dot{V}	volumetric flow rate

Greek Letters

α_{Bvane}	diffuser vane setting angle
Δp	pressure difference
ρ	density
φ	flow coefficient
κ	isentropic coefficient
2θ	diffuser channel divergence angle

Subscripts

2	impeller outlet
3	diffuser outlet ($r_3/r_2 = 1.79$)
A	stage outlet
B	diffuser vane leading edge ($r_B/r_2 = 1.16$)
C	diffuser throat
D	diffuser channel exit
E	stage inlet
K	curvature

Superscripts

o	stagnation
---	------------

EXPERIMENTAL SETUP AND INSTRUMENTATION

The experiments were performed on a closed loop test rig using air. The single-stage centrifugal compressor is driven by a 440 kW DC-motor coupled to a two stage gear box. The maximum rotational speed is limited to 22,000 RPM by the shaft seal. The flow rate is controlled by a throttle. The pressure in the suction pipe was set to 960 mbar and the inlet temperature was held at 24° C. **Figure 1** shows the test rig. A flow straightener mounted in the suction pipe ensures axial flow at the stage inlet.

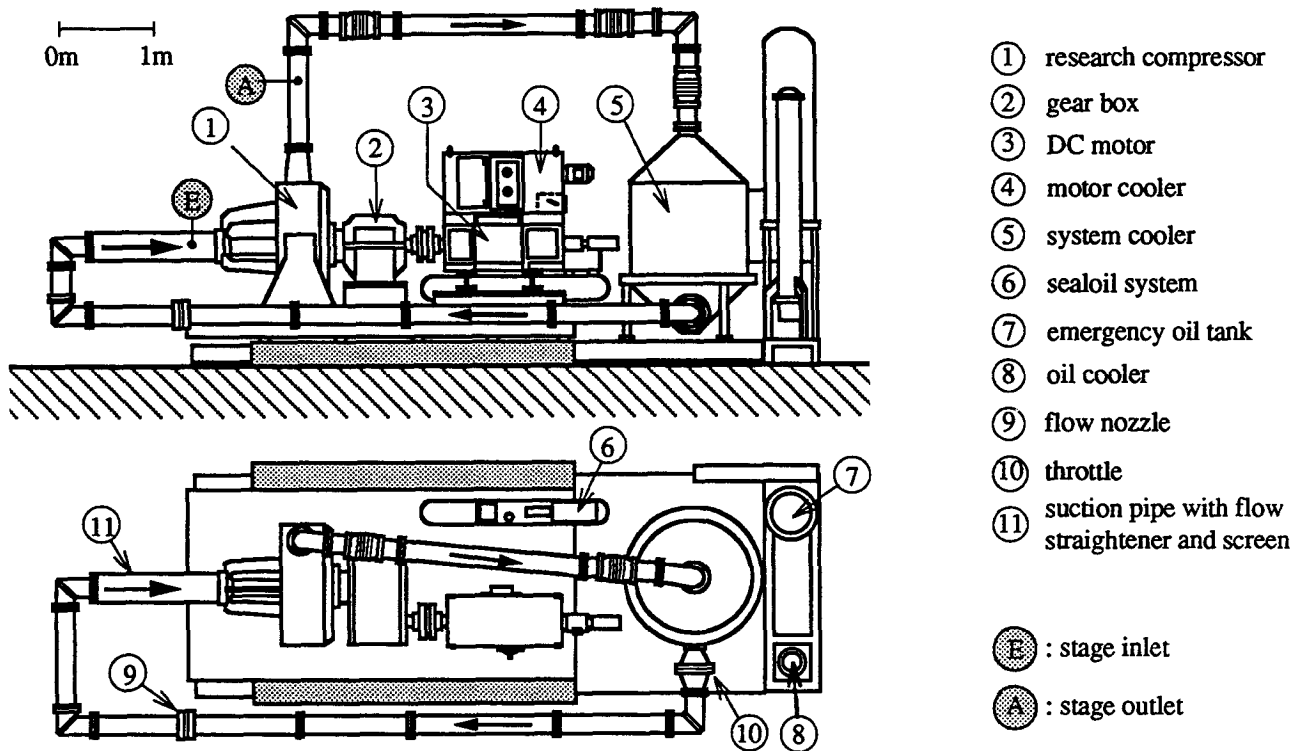


FIGURE 1: GENERAL VIEW OF THE TEST RIG

The cross-sectional view of the of the stage in Figure 2 and the picture in Figure 3 reveal more details of the compressor stage. The main data of the unshrouded impeller used in the present tests were:

impeller tip diameter d_2	280 mm
full/splitter blades	11/11 (total 22)
exit blade angle	30° back lean
exit width	17 mm

The vaned diffuser investigated consists of two parallel walls and 24 circular-arc vanes. By adjusting the diffuser vanes by turning them around a pin fixing the leading edge different diffuser configurations can be realized. The centre of the leading edge is at radius $r_B/r_2 = 1.16$. Three different diffusers were investigated by setting the vane angle $\alpha_{B \text{ vane}}$ at the leading edge to 15°, 25° and 30°. A diffuser channel is sketched in Figure 4 and the main parameters of the diffuser are listed in Table I. It is a common practice to describe radial diffusers by the area ratio AR and by the ratio of length l to inlet width h , or alternatively by the divergence angle 2θ . The relationship between 2θ and l/h is given by:

$$2\theta = 2 \operatorname{atan}\left(\frac{AR - 1}{2 l/h}\right) \quad (1)$$

TABLE I: GEOMETRIC DATA OF DIFFUSERS

$\alpha_{B \text{ vane}}$	AR_{BD}	l_{BD}/h_B	$2\theta_{BD}$	AR_{CD}	l_{CD}/h_C	$2\theta_{CD}$
15°	2.95	10.2	10.9°	2.37	6.5	12.0°
25°	2.14	5.9	11.1°	1.90	4.2	12.1°
30°	1.96	4.9	11.3°	1.79	3.7	12.2°

The radial diffuser is followed by a large toroidal collecting chamber providing a virtually uniform circumferential pressure distribution.

The overall performance of the compressor was determined by conventional wall pressure taps and temperature probes in the suction pipe and in the outlet tube. Along the casing contour as well as in the front and rear diffuser wall a large number of wall pressure taps are located. All wall-tap pressure data were taken by means of

a multichannel pressure data acquisition system with about 250 ports. The accuracy of this system is about 1 mbar. All the temperature and pressure data are collected by a μ Vax computer.

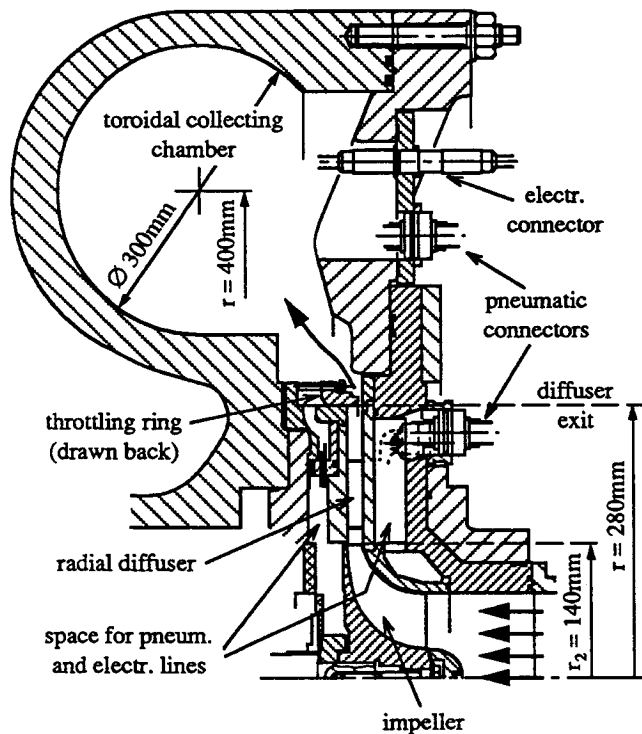


FIGURE 2: CROSS-SECTIONAL VIEW OF THE CENTRIFUGAL COMPRESSOR STAGE

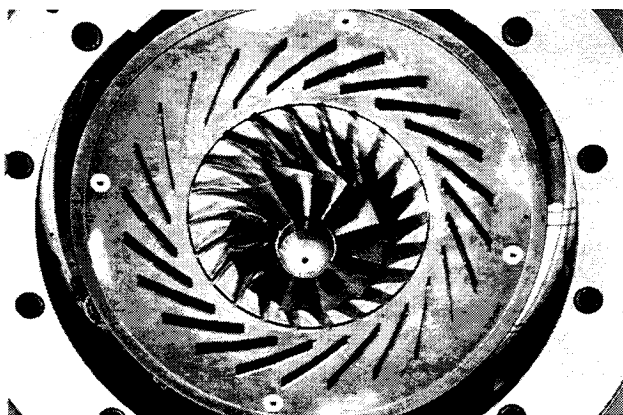


FIGURE 3: VIEW OF CENTRIFUGAL IMPELLER AND VANED RADIAL DIFFUSER (25°)

Any wall pressure fluctuations caused by flow instabilities as rotating stall or surge are detected by high frequency response pressure transducers placed in the diffuser entry region, whose signals are amplified, filtered (cut off frequency 10 kHz) and recorded on a multichannel tape. Afterwards the signals are processed using a two channel frequency analyzer. From the frequency information and the phase shift of the signals of two circumferentially displaced transducers the type of the instability (rotating stall or surge) can be diagnosed.

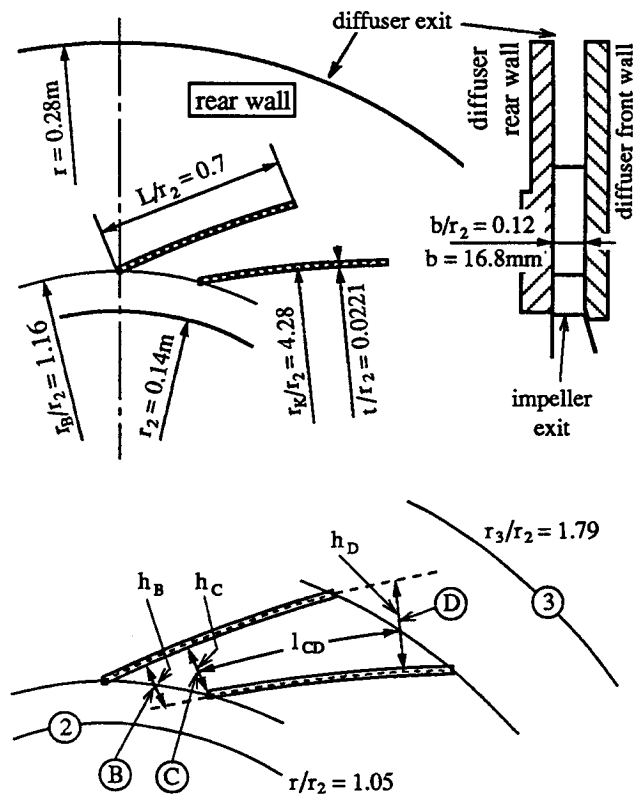


FIGURE 4: SKETCH OF THE VANED DIFFUSER

PERFORMANCE MAP

For each of the three diffuser configurations the measurements were taken at four different speeds. The rotational speed of the impeller is expressed by a peripheral Mach number Mu :

$$Mu = \frac{u_2}{\sqrt{\kappa R T_E^0}} \quad (2)$$

The dimensionless flow coefficient ϕ used instead of the volumetric flow rate \dot{V} is defined by:

$$\phi = \frac{\dot{V}}{d_2^2 u_2} \quad (3)$$

The performance map in terms of volume flow rate and total pressure ratio, with Mu and diffuser vane setting angle as parameters, are shown in Figure 5. This map will be discussed in detail below.

As can be seen, the operational range of the compressor stage can be significantly extended to lower flow rate by lowering the vane setting angle. Simultaneously the flow range (maximum flow rate - minimum flow rate) becomes smaller.

The width of the diffuser throat, which of course changes with the vane setting angle, clearly determines the maximum (or "choking") flow rate at each speed line. The minimum safely achievable flow rate is fixed by the occurrence of flow instabilities, mild surge or deep surge.

At low rotational speed, for example $Mu = 0.5$ or lower, inducer rotating stall seems to be responsible for the triggering of deep surge, Ribl and Gyarmathy (1993). Another typical problem of the impeller flow, a recirculation zone at the impeller inlet occurring at $\phi < 0.05$, affects only the onset of mild surge at low speeds in case of the 25° and 30° configurations.

At the higher rotational speeds, however, mild surge appears in the 25° and 30° configurations at higher flow rates than any of the flow disturbances associated with the impeller. On the other hand with the 15° diffuser mild surge was observed to start at a flow rate where impeller tip recirculation already existed. Therefore the diffusers play a much stronger role in limiting the stable flow range than the impeller. The observations are summarized in Table II in terms of ϕ .

The maximum achievable stage pressure ratio at any given speed is seen to increase with decreasing vane stagger angle. There are two reasons for this. Firstly, the impeller produces more head at lower flow rate ϕ as result of blade back lean. Secondly, the pressure recovery in the diffuser channel becomes higher as a result of the changes in the main geometric dimensions of the diffuser.

TABLE II: SUMMARY OF INSTABILITY TYPES OBSERVED

Speed	Diffuser Vane Setting		
	15°	25°	30°
$Mu = 0.9$	$\phi < 0.050$ impeller recirculation $\phi < 0.047$ mild surge at max. of stage characteristic $\phi = 0.046$ deep surge is triggered	$\phi < 0.057$ mild surge at max. of stage characteristic $\phi = 0.055$ deep surge is triggered	$\phi < 0.057$ mild surge at max. of stage characteristic $\phi = 0.053$ deep surge is triggered
$Mu = 0.75$	$\phi < 0.05$ impeller recirculation No mild surge $\phi = 0.037$ deep surge is triggered	$\phi < 0.054$ mild surge at max. of stage characteristic $\phi = 0.049$ deep surge is triggered	$\phi < 0.055$ mild surge at max. of stage characteristic $\phi = 0.047$ deep surge is triggered
$Mu = 0.6$	$\phi < 0.050$ impeller recirculation $\phi = 0.028$ deep surge is triggered by impeller rotating stall	$\phi < 0.050$ mild surge at max. of stage characteristic $\phi = 0.044$ deep surge is triggered	$\phi < 0.052$ mild surge at max. of stage characteristic $\phi = 0.022$ deep surge is triggered
$Mu = 0.4$	$\phi < 0.050$ impeller recirculation No mild surge $\phi = 0.028$ deep surge is triggered by impeller rot. stall	$\phi < 0.050$ impeller recirculation $\phi < 0.050$ mild surge $\phi = 0.028$ deep surge is triggered by impeller rot. stall	$\phi < 0.050$ impeller recirculation $\phi < 0.050$ mild surge $\phi = 0.028$ deep surge is triggered by impeller rot. stall

stagnation pressure ratio

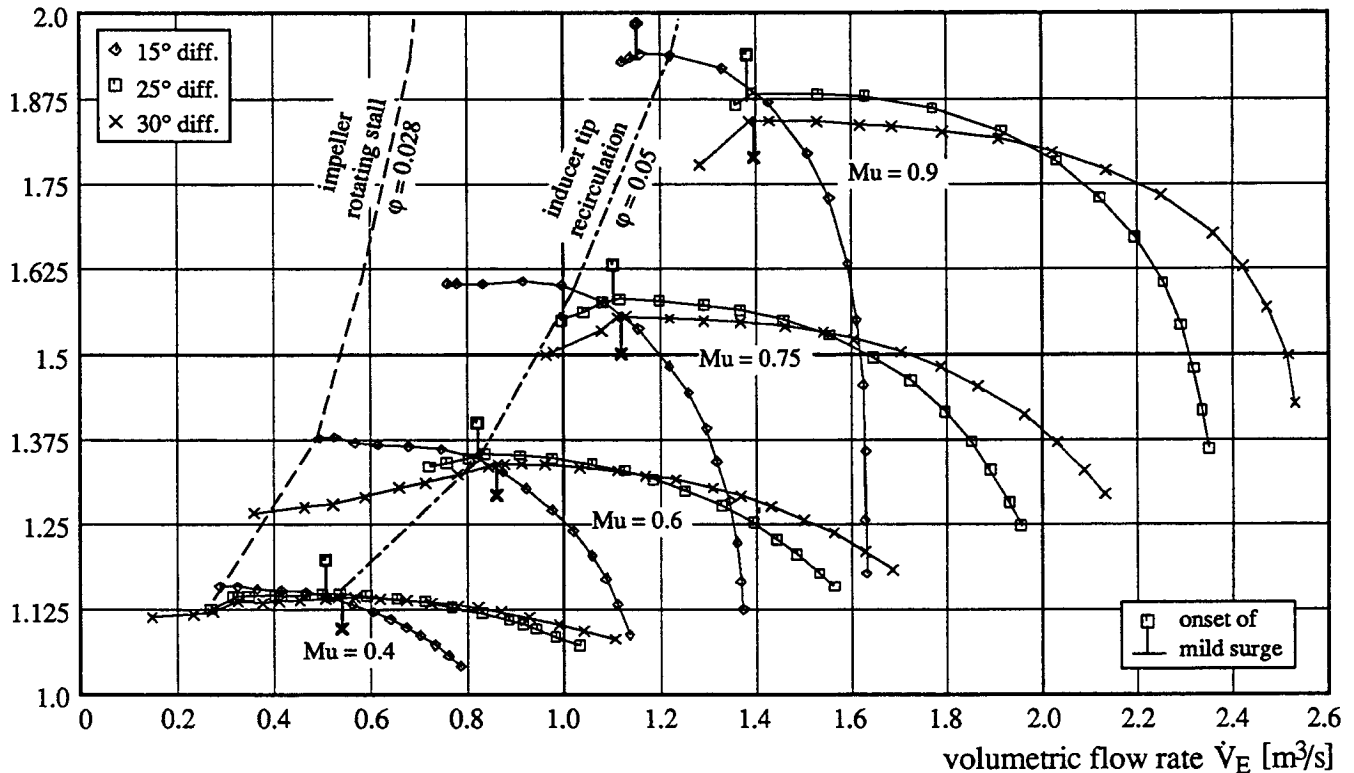


FIGURE 5: PERFORMANCE MAP

As mentioned above, the stability limit for mild surge regularly occurs, in accordance with Greitzer's theory, at the flow rate giving maximum pressure rise in the overall stage. Here the slope of the stage characteristic is zero. Figure 6 shows the time traces of static pressure at stage inlet (PVE), at diffuser entry (PDE1) and at diffuser outlet (PDA). At the top of the figure the time mean flow rate is indicated. At diffuser entry (PDE1) high-frequency pressure fluctuations associated with the impeller are dominant. If the flow rate \dot{V} falls short of $1.10 \text{ m}^3/\text{s}$ (the value corresponding to the maximum of the stage characteristic at $Mu = 0.75$) a periodic pressure oscillation arises as seen in the traces PVE and PDA. The frequency of 19Hz corresponds to an acoustic resonance of the whole compression system and remains the same at other rotational speeds. This oscillation is synchronous over the circumference. For these reasons these pressure fluctuations have to be interpreted as mild surge. Further decreasing the flow rate results in an increase of the amplitude of the pressure fluctuations at constant frequency. The accompanying flow oscillations have been analysed by Ribi and Gyarmathy (1993).

PRESSURE FIELDS IN THE DIFFUSER

About 60 static wall pressure taps distributed over the shroud side of the radial diffuser provide wall pressure distributions. Figure 7 shows the wall pressure fields of three different operating conditions. These measured distributions correspond to those calculated and described in Dalbert et al. (1993).

At high flow rate (Figure 7, top) there is a strong local acceleration when the steep inlet flow turns into the diffuser channels. In the semi-vaneless space a pressure gradient acts against the vanes. Minimum pressure exists on the outward facing side of the vanes (which is normally referred to as the "pressure side"). Local flow separation behind the leading edge on the pressure side may exist. Downstream of the throat the flow becomes more and more one-dimensional.

At medium and low flow rate (Figure 7, centre and bottom) there is a continuous and regular pressure rise in the semi-vaneless space and in the channel. A local pocket of low pressure exists on the suction side near the leading edge. This indicates a turning of the incident flow from a more tangential direction into the channel.

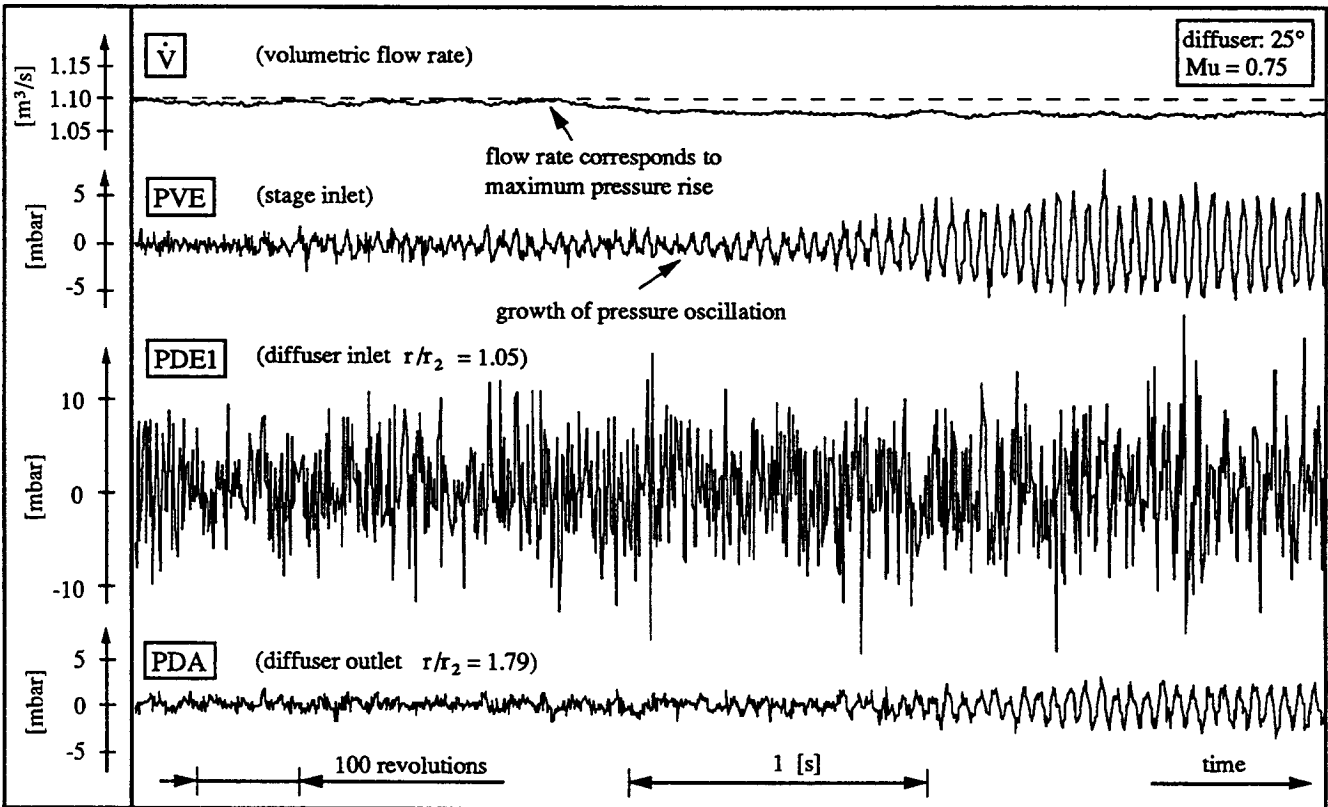


FIGURE 6: TYPICAL PRESSURE TRACES DURING THE ONSET OF MILD SURGE

The static pressure field in the vaneless and semi-vaneless space is very sensitive to flow rate. At low flow rate the stationary static pressure field set up by the vanes is most uneven in circumferential direction. This may stimulate impeller blade vibration.

COMPONENT AND SUBCOMPONENT CHARACTERISTICS

Since mild surge occurs at the maximum of the stage overall pressure rise characteristic, it is interesting to examine the characteristics of each component and subcomponent of the compressor in order to determine which components influence the stage characteristics significantly. First the stage is divided into the components impeller, diffuser and collector. Afterwards the diffuser is subdivided into vaneless and semi-vaneless space, diffuser channel and vaneless space downstream of the channels.

The characteristics obtained from an analysis of the pressure measurements are given for each component in a dimensionless form as:

$$D_p = \frac{\Delta p}{\rho_E u_2^2 / 2} \quad (4)$$

Here Δp is the static pressure rise in the component. The static pressures in planes 2, C, D and 3 as indicated in figure 4 are mean values averaged over several tappings. In the plane C and D the wall pressure data is averaged along the line h_C and h_D , respectively. In plane 2 and 3 the data is averaged in circumferential direction.

In a similar way to Dean (1974) or Japikse (1984) a stability parameter of the component is obtained as $\partial D_p / \partial \phi$. This parameter corresponds to the slope of the dimensionless pressure rise characteristic of the component.

The classical (Greitzer) stability theory identifies the stability limit with the peaking of the total-to-static pressure rise characteristic of the stage. Since the flow velocity at the stage inlet (E) is low the difference between total and static pressure in plane E is small. Therefore it is of little importance if the total-to-static or the static-to-static pressure rise characteristic of the stage is used.

Taking the latter approach for simplicity, both the impeller and the diffuser characteristics are taken static-to-static. The characteristics of the diffuser subcomponents and of the collector are static-to-static in both cases.

As discussed in detail by Greitzer (1981), positively sloped characteristics are to be avoided generally. Of particular interest is the identification of those "culprit" components or subcomponents which contribute a positively sloped characteristic and of those stabilizing components which have a strongly negative slope. This analysis and identification have been carried out for the configurations tested.

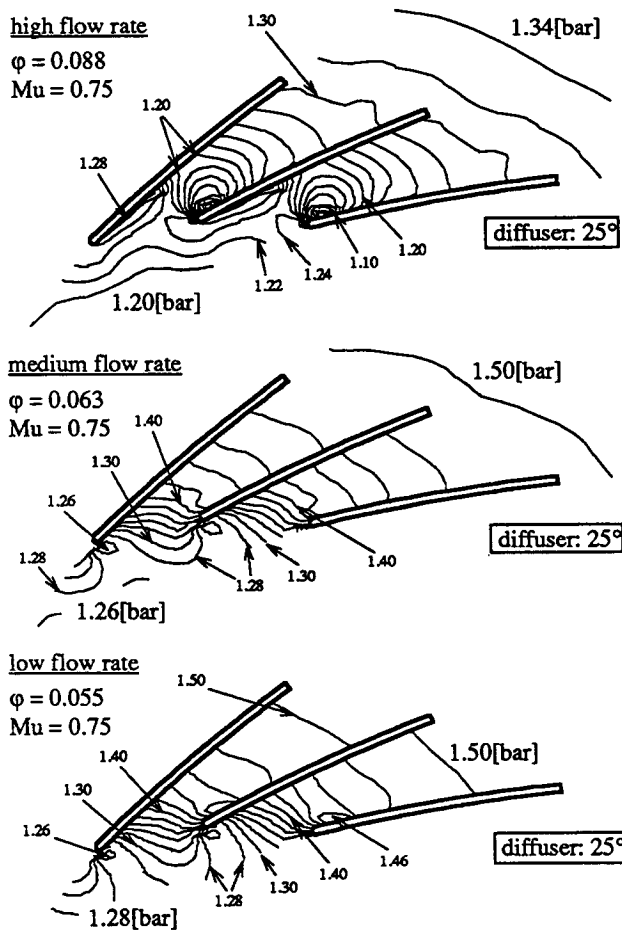


FIGURE 7: ISOBARS WITHIN THE 25° DIFFUSER AT THREE DIFFERENT OPERATING CONDITIONS

Figure 8, upper part, shows the D_p characteristics of the individual components for one configuration. The lower part shows the D_p slope. The impeller has a stabilizing

effect over the whole stable operating range. Since the impeller has 30° back-swept blades, this observation is plausible. The diffuser has a strong stabilizing effect at high flow rate but is slightly destabilizing at low flow rate. The collector acts as a destabilizer at high flow rate but is neutral at medium and low flow rates.

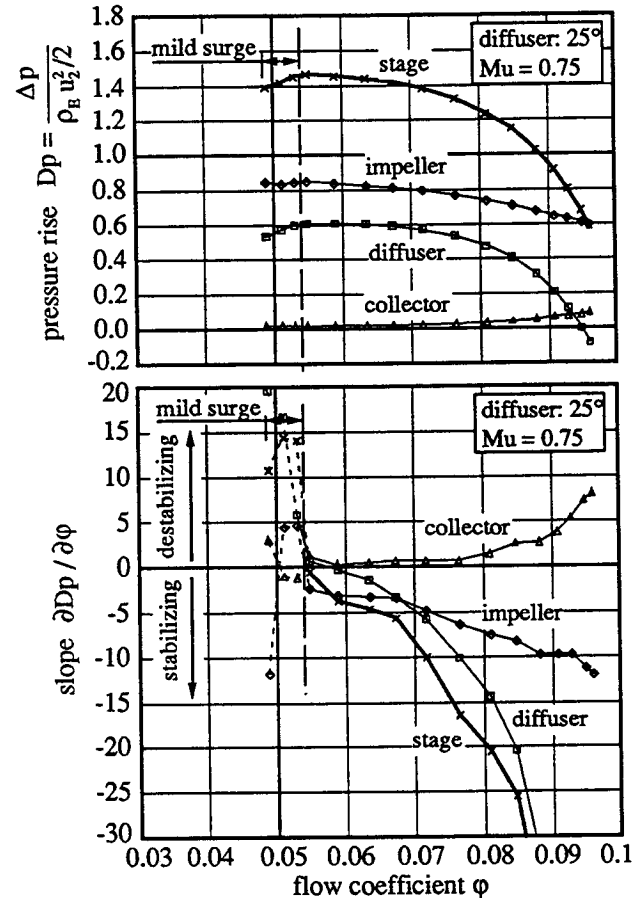


FIGURE 8: CHARACTERISTICS OF THE COMPONENTS AND SLOPES OF THE CHARACTERISTICS (WITH 25° DIFFUSER)

The influence of the rotational speed on the slopes of the characteristics of the stage, the impeller and the 25° diffuser is documented in Figure 9. Instabilities set in at zero stage slope. While the slope for the impeller is almost independent of the peripheral Mach number Mu , there is a dependence for the diffuser. At low speed the diffuser is stabilizing over the whole stable operating range of the stage. With increasing Mu the diffuser acts more and more destabilizing at low flow rate.

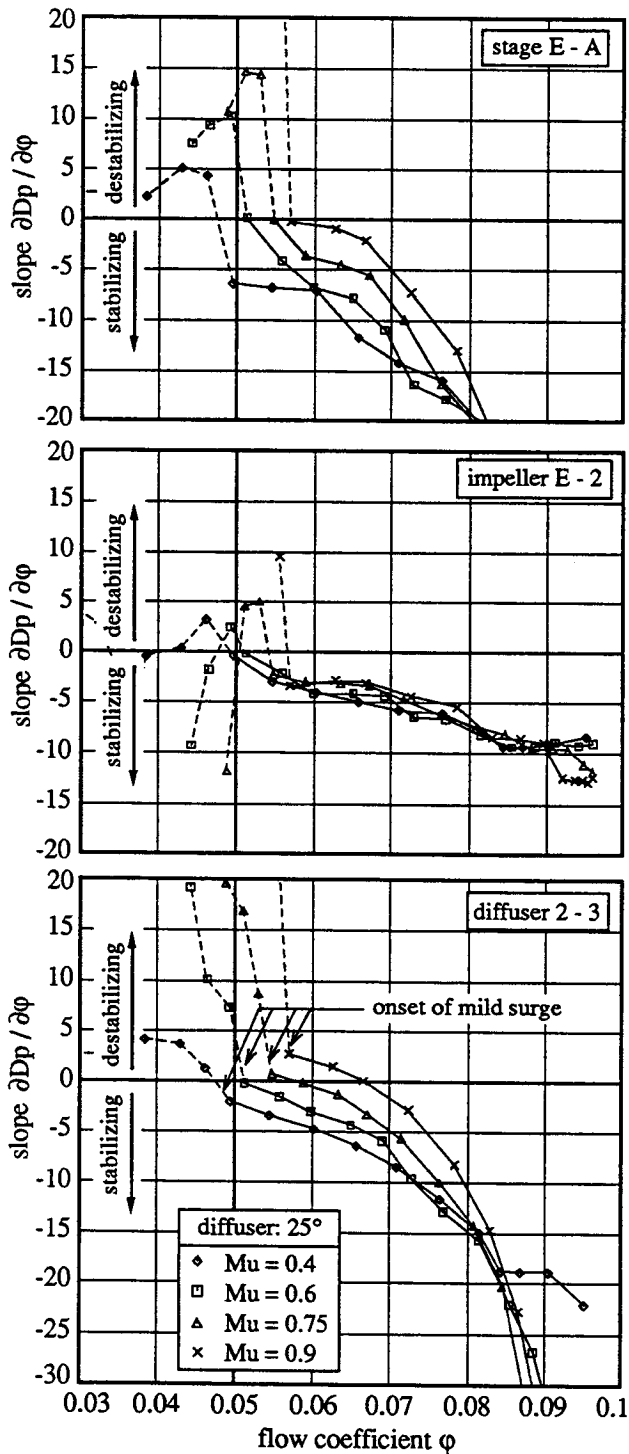


FIGURE 9: SLOPE OF THE STAGE, IMPELLER AND DIFFUSER CHARACTERISTICS (WITH 25° DIFFUSER) AT DIFFERENT SPEEDS

Figure 10 gives the slopes of the impeller and diffuser characteristics for the three different stages at $Mu = 0.9$. Since the same impeller was used in the three cases there are no differences in the impeller characteristics. But with the 15° diffuser, where stable stage operation with inducer tip recirculation was possible ($\phi < 0.05$), the impeller acts destabilizing, whereas in this stage the diffuser is always stabilizing. With the other two stages (25° and 30°) the situation is reversed. Here the impeller is always stabilizing but the diffusers are destabilizing at reduced flow rate. Of course at high flow rate the diffusers are also stabilizing.

In the same manner, the diffuser can be analysed in sections. This reveals the contribution of the diffuser subcomponents to the characteristic slope. For three diffuser elements, the diffuser inlet (comprising the vaneless and semi-vaneless space, 2-C), the diffuser channel (C-D) and the vaneless space downstream the channel (D-3), the characteristics D_p are shown in Figure 11 for the stage with the 25° diffuser. The slopes are plotted in Figure 12.

The diffuser inlet appears to be the most stabilizing element of the stage over a wide flow range. This agrees with Japikse (1984). But with decreasing flow rate this element acts less and less stabilizing, especially if Mu is high.

The diffuser channel is always destabilizing, except at high flow rate and high Mu where the flow is accelerating at the channel entry (throat). No significant effect of Mach number on the slope of the characteristics can be seen.

The vaneless space downstream of the diffuser channel is slightly destabilizing.

Figure 13 and 14 show the diffuser element D_p characteristics for the 15° and the 30° diffuser, respectively. Essentially the same trends appear. The channel is mainly destabilizing, the vaneless space downstream the channel is also destabilizing. The diffuser's entry region is stabilizing over a wide range, but the strength of this effect decreases during throttling. The example of the 30° diffuser (Figure 14) shows that this element is also able to act destabilizing at reduced flow rate.

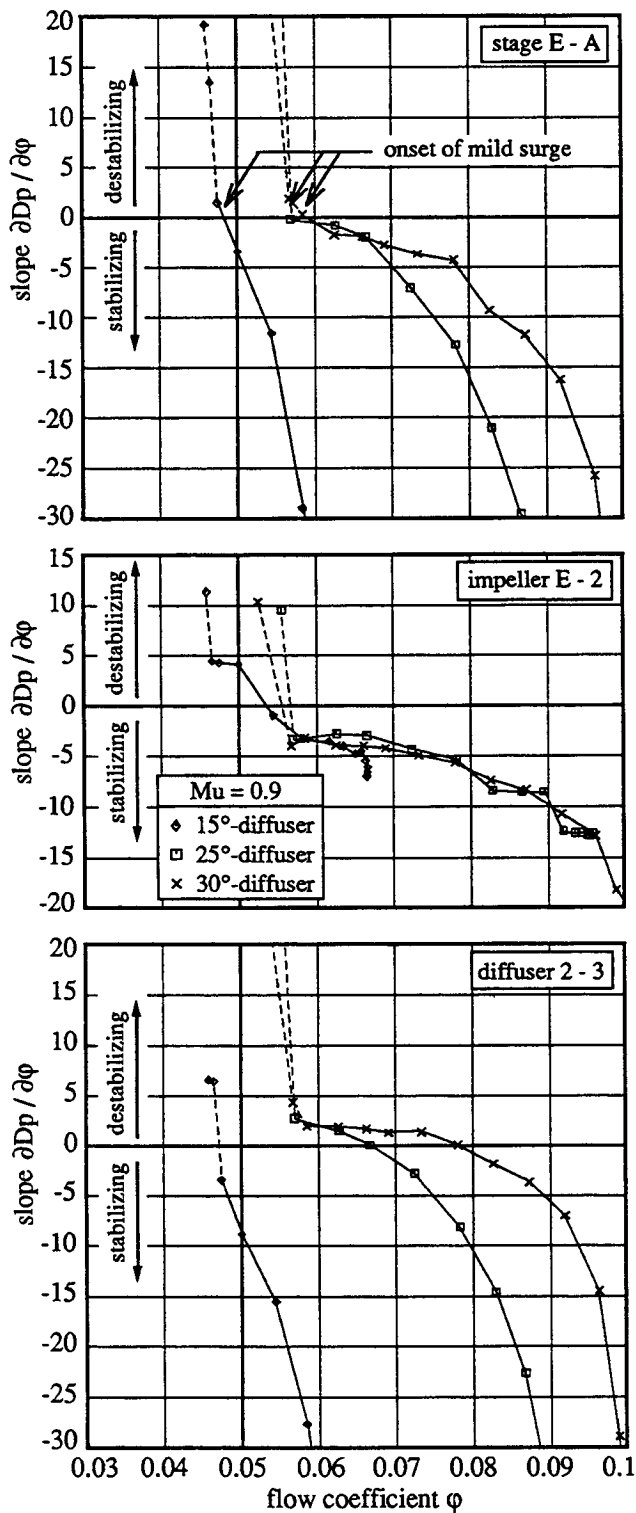


FIGURE 10: SLOPE OF THE STAGE, IMPELLER AND DIFFUSER CHARACTERISTICS FOR THE THREE DIFFUSER VANE SETTINGS, AT $\text{Mu} = 0.9$

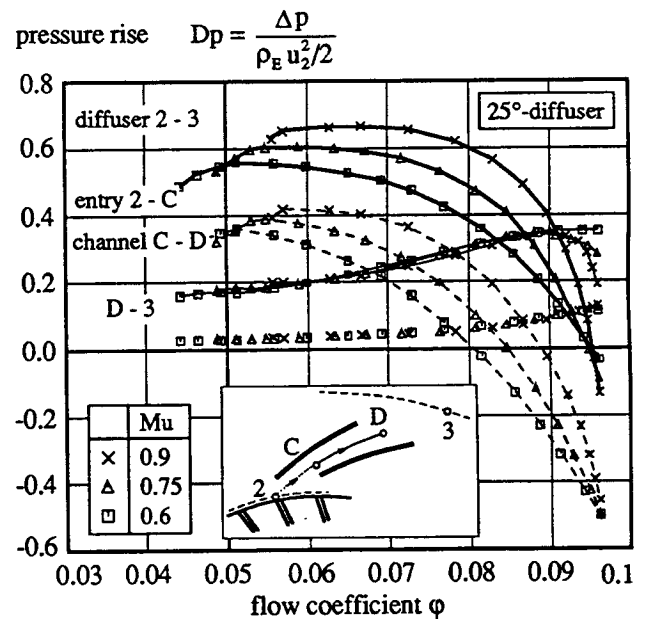


FIGURE 11: CHARACTERISTICS OF THE 25° DIFFUSER AND ITS SUBCOMPONENTS AT DIFFERENT SPEEDS

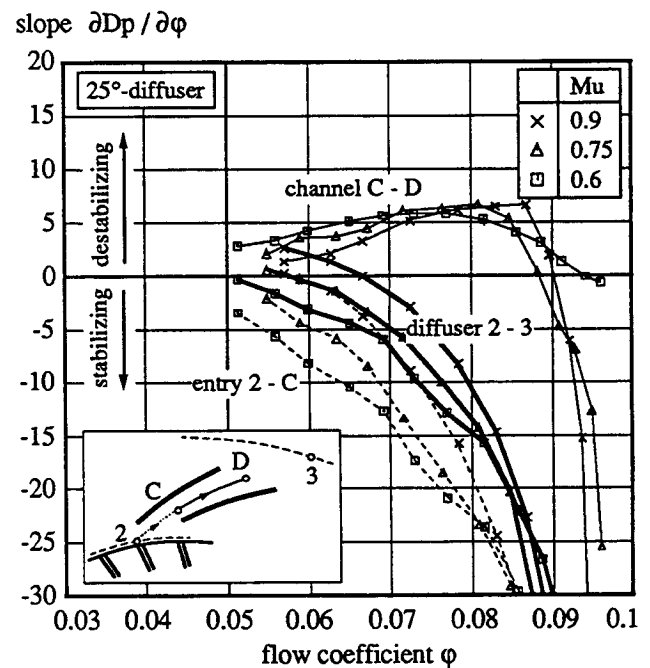


FIGURE 12: SLOPES OF THE CHARACTERISTICS OF THE 25° DIFFUSER AND ITS SUBCOMPONENTS AT DIFFERENT SPEEDS

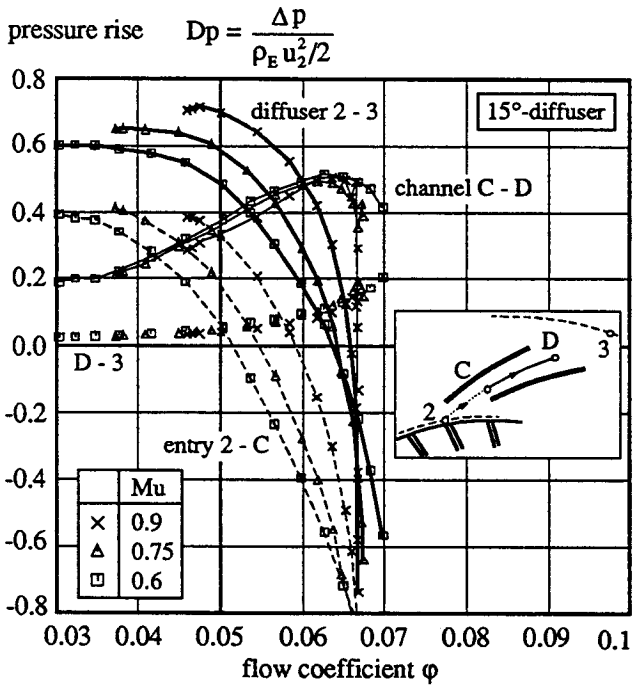


FIGURE 13: CHARACTERISTICS OF THE 15° DIFFUSER AND ITS SUBCOMPONENTS AT DIFFERENT SPEEDS

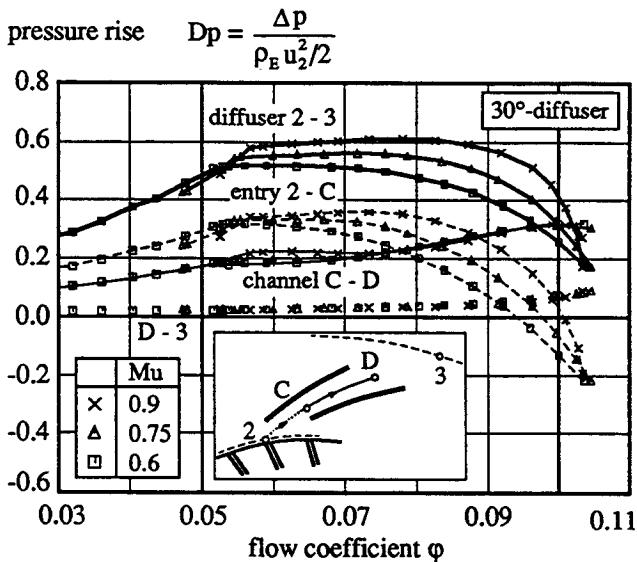


FIGURE 14: CHARACTERISTICS OF THE 30° DIFFUSER AND ITS SUBCOMPONENTS AT DIFFERENT SPEEDS

Of great interest is the observation that the diffuser channel with the smallest throat area and with the longest

channel (highest l/h_C) having the highest area ratio AR, is the most destabilizing one.

DIFFUSER CHANNEL PERFORMANCE

The pressure recovery in the diffuser channel is defined as:

$$C_p = \frac{\Delta p_{C-D}}{p_{C-PC}^0} \quad (5)$$

It differs from Dp in referring the pressure rise to the actual inlet velocity head. This pressure recovery coefficient is usually compared with those of Reneau et al. (1967) and Runstadler et al. (1975) who tested different diffuser geometries. It is well known that inlet blockage is a main parameter. Therefore the pressure recovery coefficient is plotted versus the diffuser throat blockage Bl_C in Figure 15. Similar plots are given in the literature (e.g. Japikse and Osborne (1986), Clements (1987), Verdonk (1978)). The blockage definition used is:

$$Bl_C = 1 - \frac{A_{eff} C}{A_C} \quad (6)$$

The area $A_{eff} C$ effectively used by the flow is calculated using the diffuser throat static pressure, the stagnation pressure measured in the diffuser vane leading edge (by means of a pitot probe) and the continuity equation.

The present data points in the vertical bands correspond to high flow rate. The more horizontal portion corresponds to operating conditions between best efficiency and surge. The latter data show approximately the level indicated by Reneau or Runstadler, but the tendencies are different. Unfortunately their laboratory data do not cover the interesting range for most centrifugal compressor diffusers in terms of geometry or blockage. The slight increase in pressure recovery at increasing blockage is supposed to be due to two effects. Firstly, since the pitot probe only indicates the stagnation pressure in the flow core, any changes in the stagnation pressure *distribution* are not recognized correctly. This may result in an overestimation of the pressure recovery. Secondly, the pressure recovery in the channel of a radial diffuser is caused not only by deceleration but by blade forces (deflection) too. This may in fact increase the recovery coefficient.

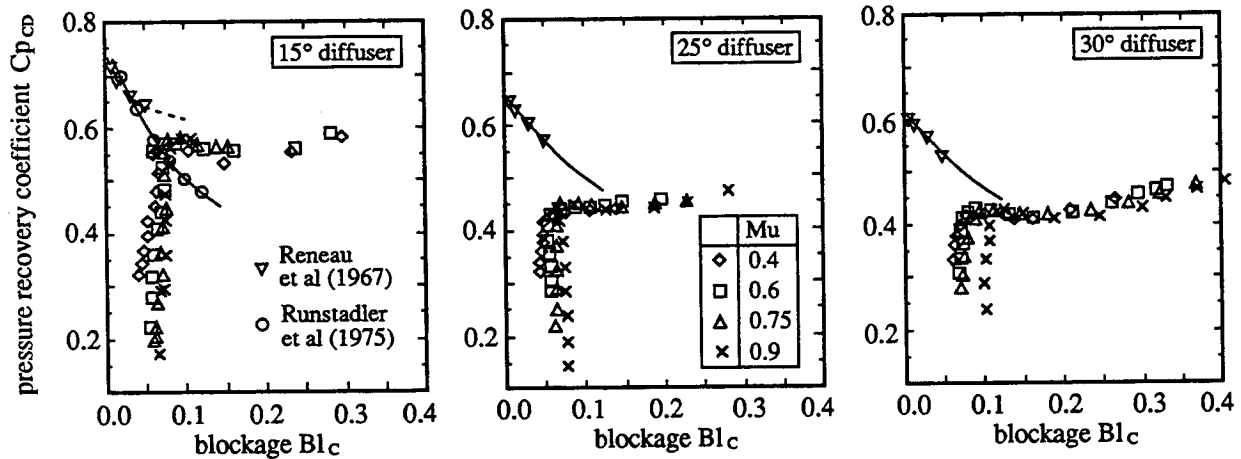


FIGURE 15: CHANNEL PRESSURE RECOVERY C_{pC-D} VS. DIFFUSER THROAT BLOCKAGE Bl_c

Channels with higher AR and higher l/h_c exhibit higher recovery coefficients in the horizontal portion in Figure 15 (reduced flow rate). This trend is in agreement with laboratory diffuser data. For comparison the geometries of the diffuser channels are plotted in the diffuser map of Reneau et al. (1967) in Figure 16.

There exists a relationship between the channel pressure rise D_{pC-D} and the channel pressure recovery coefficient C_{pC-D} as:

$$D_{pC-D} = C_{pC-D} \frac{p^o - p_c}{\rho_E u_2^2 / 2}$$

The fraction term represents the dimensionless dynamic pressure in the diffuser throat. For a given diffuser inlet geometry, especially a given throat area, its dependence on flow rate is fixed and shown in Figure 17 as the top curve. Using the D_{pC-D} curve plotted in Figure 11 the above relationship yields the curve C_{pC-D} . This is seen to fall short of the theoretical value $C_{pC-D,AR}$ calculated from the area ratio. A geometric increase in AR will normally increase C_p and D_p and act toward destabilization.

Note that the ordinate of the curve D_{pC-D} and the normalized pressure head curve is a direct measure of the utilization of impeller exit velocity in the channel part of the diffuser. This ratio appears to be fairly constant over flow rate, except for the deterioration seen at high flow.

Summarizing, the surge line movements connected with geometrical changes of the diffuser channel reported in the literature (Japikse (1984), Clements and Artt (1987)) can be understood as the consequence of basic physical

mechanisms of diffusing flow in the radial diffuser. Thereby the general observation that the radial diffuser affects the surge line (Came and Bellamy 1982) is substantiated. Diffusers designed for low pressure recovery result in an improved stability of the stage whereas diffusers for high pressure recovery result in smaller flow ranges.

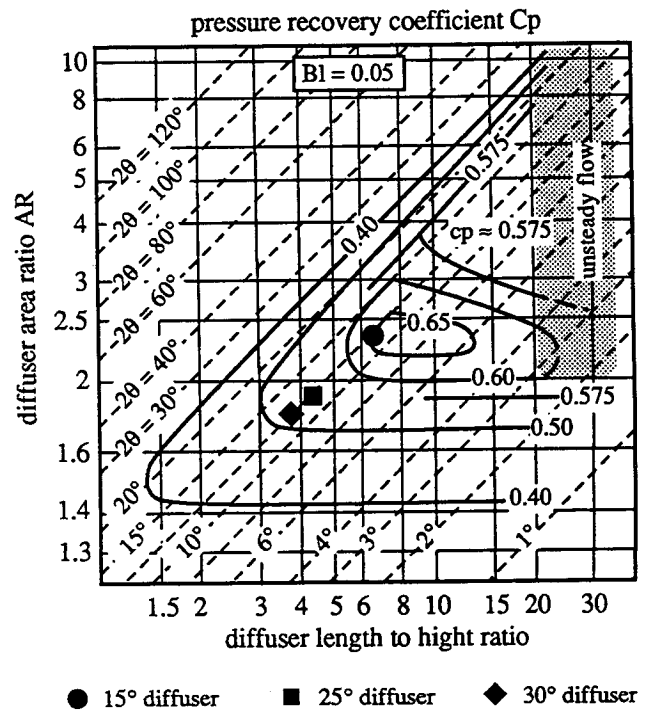


FIGURE 16: COMPARISON OF DIFFUSER CHANNEL GEOMETRY

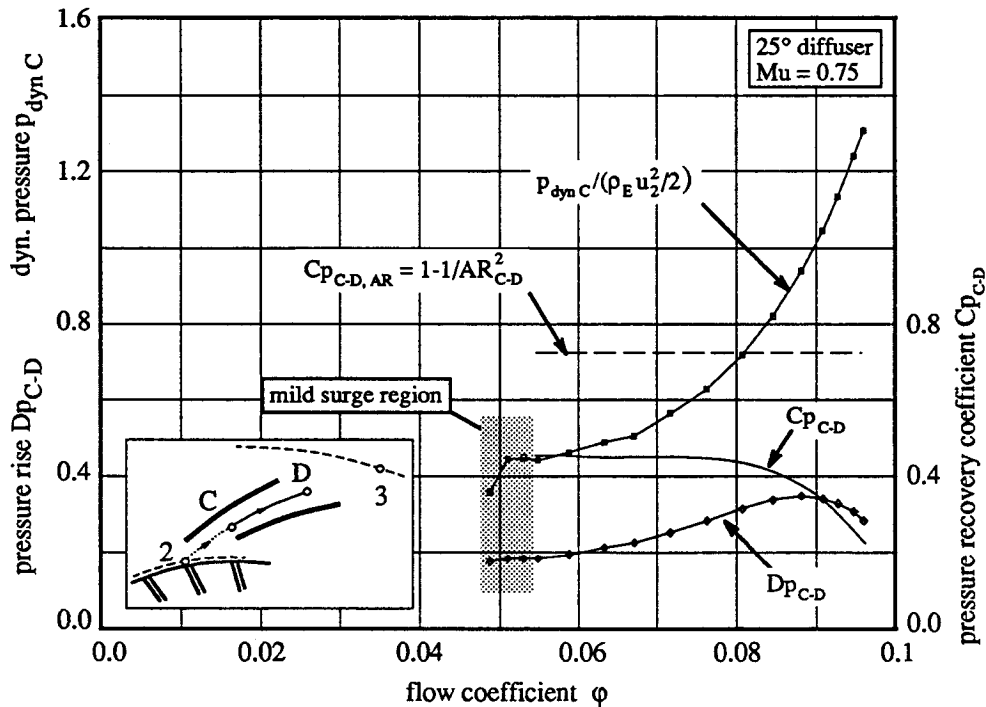


FIGURE 17: CONVERSION OF DYNAMIC PRESSURE $P_{DYN C}$ IN THE DIFFUSER CHANNEL

CONCLUSIONS

- Mild surge, as a dynamic instability of the compression system, arises at the flow rate giving the maximum overall stage pressure rise characteristic (zero slope), in perfect compliance with Greitzer's stability theory for high B-parameter values.
- The static wall pressure field in the vaneless and semi-vaneless space as well as slightly downstream of the diffuser throat is very sensitive to flow rate.
- The backswept impeller is a typically stabilizing stage element. With inlet recirculation the impeller becomes destabilizing.
- The diffuser entry region is a strong stabilizing sub-component over a wide flow range. This stabilizing influence decreases as the flow is reduced. This is the influence that mainly determines the stability limit.
- The diffuser channels play an inherently destabilizing role. The relationship of diffuser geometry and channel pressure recovery with the strength of the destabilizing effect of the channels substantiates experiments published in the literature showing surge line movements caused by changes in the diffuser channel geometry.
- With adjustable fixed-length diffuser vanes the higher total pressure ratios are obtained with lower vane stagger angle.

ACKNOWLEDGEMENTS

The Authors would like to thank the Swiss Kommission für die Förderung der Wissenschaftlichen Forschung (KWF) for the financial support and ABB Turbo Systems, Sulzer Escher Wyss, Sulzer Innotec and Sulzer Brothers Winterthur for their technical cooperation and their financial support. The authors wish to thank Mrs. D. Aeppli for typewriting this manuscript.

REFERENCES

- Abdelhamid, A.N., "Effects of Vaneless Diffuser Geometry on Flow Instability in Centrifugal Compression Systems," *Canadian Aeronautics and Space Journal*, Vol. 29, No. 3, 1983, pp. 259 - 266.
- Amann, C.A., Nordenson, G.E., Skellenger G.D., "Casing Modification for Increasing the Surge Margin of a Centrifugal Compressor in an Automotive Turbine Engine," *ASME Journal of Engineering for Power*, Vol. 97, 1975, pp. 329 - 336.
- Ariga, I., Masuda, S., Ookita, A., "Inducer Stall in a Centrifugal Compressor With Inlet Distortion," *ASME Journal of Turbomachinery*, Vol. 109, 1987, pp. 27 - 35.
- Baghdadi, S., McDonald, A.T., "Performance of Three Vaned Radial Diffusers With Swirling Transonic Flow,"

ASME *Journal of Fluids Engineering*, Vol. 97, 1975, pp. 155 - 173.

Came, P.M., Bellamy, A.G., "Design and performance of advanced large turbochargers," IMechE C37/82, 1982.

Came, P.M., Herbert, M.V., "Design and experimental performance of some high pressure ratio centrifugal compressors," AGARD, CP-282, Paper No. 15, 1980.

Clements, W.W., Artt, D.W., "The influence of diffuser channel geometry on the flow range and efficiency of a centrifugal compressor," *Proceedings of the Institution of Mechanical Engineers*, Vol. 201, 1987, pp. 145 - 152.

Clements W.W., "A theoretical and experimental study of diffusion levels in centrifugal compressor stage," Ph.D Thesis, University of Belfast, 1987.

Dalbert, P., Gyarmathy, G., Sebestyen, A., "Flow Phenomena in a Vaned Diffuser of a Centrifugal Stage," to be presented at the ASME Conference in Cincinnati, 1993.

Dean, R.C., "The Fluid Dynamic Design of Advanced Centrifugal Compressors," Lecture Notes, Von Karman Institute, Brussels, March 1974.

Dean, R.C., Young, L.R., "The Time Domain of Centrifugal Compressor and Pump Stability and Surge," *ASME Journal of Fluids Engineering*, Vol. 99, 1977, pp. 53 - 63.

Dutton, J.C., Piemsomboon, P., Jenkins, P.E., "Flowfield and Performance Measurements in a Vaned Radial Diffuser," *ASME Journal of Fluids Engineering*, Vol. 108, 1986, pp. 141 - 147.

Elder, R.L., Gill, M.E., "A Discussion of the Factors Affecting Surge in Centrifugal Compressors," *ASME Journal of Engineering for Gas Turbines and Power*, Vol. 107, 1985.

Emmons, H.W., Pearson, C.E., Grant, H.P. "Compressor Surge and Stall Propagation," *ASME Transactions*, Vol. 77, 1955, pp. 455 - 469.

Filipenco, V.G., "Experimental Investigation of Flow Distortion Effects on the Performance of Radial Discrete-Passage Diffusers", GTL Report 206, Gas Turbine Laboratory, MIT, 1991.

Fink, D.A., Cumpsty, N.A., Greitzer, E.M., "Surge Dynamics in a Free-Spool Centrifugal Compressor System," *ASME Paper 91-GT-31*, 1991.

Frigne, P., Van Den Braembussche, R., "Distinction Between Different Types of Impeller and Diffuser Rotating Stall in a Centrifugal Compressor With Vaneless Diffuser," *ASME Journal of Engineering for Gas Turbines and Power*, Vol. 106, 1984, pp. 468 - 474.

Greitzer, E.M., "The Stability of Pumping Systems - The Freeman Scholar Lecture," *ASME Journal of Fluids Engineering*, Vol. 103, 1981, pp. 193 - 242.

Gysling, D.L., Dugundji, J., Greitzer, E.M., Epstein, A.H., "Dynamic Control of Centrifugal Compressor Surge Using Tailored Structures," *ASME Paper 90-GT-122*, 1990.

Jansen, M., "Untersuchungen an beschauelten Diffusoren eines hochbelasteten Radialverdichters," Ph.D Thesis, University of Hannover, 1982.

Jansen, W., "Rotating Stall in a Vaneless Diffuser," *ASME Journal of Basic Engineering*, Vol. 86, 1964, pp. 750 - 758.

Japikse, D., "A critical evaluation of stall concepts for centrifugal compressors and pumps - Studies in component performance, part 7," *ASME-Conference on stall and surge in compressors and pumps*, 1984.

Japikse, D., Osborne, C., "Optimization of Industrial Centrifugal Compressors Part 6B: Studies in Component Performance - Laboratory Development of Eight Stages From 1972 to 1982," *ASME Paper 86-GT-222*, 1986.

Japikse, D., "The Influence of Diffuser Inlet Pressure Fields on the Range and Durability of Centrifugal Compressor Stages," AGARD CP-282, Paper No. 13, 1980.

Kämmer, N., Rautenberg, M., "A Distinction Between Different Types of Stall in a Centrifugal Compressor Stage," *ASME Journal of Engineering for Gas Turbines and Power*, Vol. 108, 1986, pp. 83 - 92.

Kämmer, N., Rautenberg, M., "An Experimental Investigation of Rotating Stall Flow in a Centrifugal Compressor," *ASME Paper 82-GT-82*, 1982.

Kenny, D.P., "A Comparison of the Predicted and Measured Performance of High Pressure Ratio Centrifugal Compressor Diffusers," *ASME Paper 72-GT-54*, 1972.

Krain, H., "A Study on Centrifugal Impeller and Diffuser Flow," *ASME Journal of Engineering for Power*, Vol. 103, 1981.

Pinsley, J.E., Guenette G.R., Epstein, A.H., Greitzer, E.M., "Active Stabilization of Centrifugal Compressor Surge," *ASME Paper 90-GT-123*, 1990.

Reneau, L.R., Johnston, J.P., Kline, S.J., "Performance and Design of Straight, Two-Dimensional Diffusers," *ASME Journal of Basic Engineering*, Vol. 89, 1967, pp. 141 - 150.

Ribi, B., Gyarmathy, G., "Impeller Rotating Stall as a Trigger for the Transition from Mild to Deep Surge in a Subsonic Centrifugal Compressor," to be presented at the ASME Conference in Cincinnati, 1993.

Rieder, M., "Das instationäre Strömungsverhalten von Radialverdichterstufen mit langsamläufigen Laufrädern und schaukellosen Diffusoren im Pumpgrenzbereich," Ph.D Thesis, University of Stuttgart, 1987.

Rodgers, C., "The Performance of Centrifugal Compressor Channel Diffusers," ASME Paper 82-GT-10, 1982.

Runstadler, P.W., Dolan, F.X., Dean, R.C., "Diffuser Data Book," Creare Technical Note TN-186, 1975.

Simon, J.S., Valavani, L., Epstein, A.H., Greitzer, E.M., "Evaluation of Approaches to Active Compressor Surge Stabilization," ASME Paper 92-GT-182, 1992.

Stein, W., Rautenberg, M., "Analysis of Measurements in Vaned Diffusers of Centrifugal Compressors," ASME Paper 87-GT-170, 1987.

Toyama, K., Runstadler, P.W., Jr., Dean, R.C., Jr., "An Experimental Study of Surge in Centrifugal Compressors," *ASME Journal of Fluids Engineering*, Vol. 99, 1977, pp. 115 - 131.

Verdonk, G., "Vaned Diffuser Inlet Flow Conditions for a High Pressure Ratio Centrifugal Compressor," ASME Paper 78-GZ-50, 1978.

Yoshinaga, Y., Gyobu, I., Mishina, H., Koseki, F., Nishida, H., "Aerodynamic Performance of a Centrifugal Compressor With Vaned Diffusers," *ASME Journal of Fluids Engineering*, Vol. 102, 1980, pp. 486 - 493.